

Elsevier required licence: © <2018>. This manuscript version is made available under the CC-BY-NC-ND 4.0 license <http://creativecommons.org/licenses/by-nc-nd/4.0/>  
The definitive publisher version is available online at

[\[https://www.sciencedirect.com/science/article/pii/S0003682X17306564?via%3Dihub\]](https://www.sciencedirect.com/science/article/pii/S0003682X17306564?via%3Dihub)

Reducing low frequency tonal noise in large ducts  
using a hybrid reactive-dissipative silencer

Paul Williams<sup>a\*</sup>, Ray Kirby<sup>b</sup>, James Hill<sup>a</sup>, Mats Åbom<sup>c</sup>, Colin Malecki<sup>a</sup>

<sup>a</sup> AAF Ltd., Bassington Lane, Cramlington, Northumberland, NE23 8AF, U.K.

<sup>b</sup> Centre for Audio, Acoustics and Vibration, University of Technology, Sydney, NSW,  
2007, Australia.

<sup>c</sup> KTH, The Marcus Wallenberg Laboratory (MWL), SE-100, 44 Stockholm, Sweden.

## Abstract

Noise generated by fans or turbines normally consists of a combination of narrow and broadband noise. To lower transmitted noise levels, it is attractive to use a combination of reactive and dissipative elements. However, this approach presents a number of challenges for larger systems. This is because reactive elements are normally only effective up to the frequency at which the first higher order modes cuts on in the duct. For larger systems, this means that reactive elements work only in the low, and often very low, frequency range, whereas dissipative elements generally work well in the medium to high frequency range. This can cause noise problems in the low to medium frequency range in larger systems. This article presents an alternative approach for delivering noise attenuation over the low to medium frequency range that is suitable for application in larger duct systems. This approach takes advantage of those splitter silencer designs commonly used in larger systems to integrate a reactive element into the splitter design. This delivers a hybrid splitter that uses a combination of dissipative and reactive elements so that the reactive element partitions the main airway. This has the advantage of introducing a quasi-planar transverse sound pressure field for each resonator in the low to medium frequency range, including frequencies above the first cut-on. It is demonstrated using predictions and measurements taken for a number of example silencers, that this approach enables reactive elements to work over an extended low to medium frequency range, including at frequencies above the first cut-on mode in the main duct. Accordingly, it is shown that a hybrid dissipative-reactive splitter design is capable of delivering improved levels of attenuation in the crucial low to medium frequency range.

**Keywords:** Low frequency noise, large ducts, hybrid silencer

## 1. Introduction

The control of noise emissions from power generating equipment is normally addressed using passive noise control techniques such as reactive and dissipative sound attenuators. This is because alternative techniques such as active noise control are not well suited to the harsh environmental conditions and large geometries often encountered in power generating systems. Passive techniques tend to work well for smaller systems, such as exhaust systems for internal combustion engines used in the automotive industry. This is because sound propagation in automotive exhaust and intake pipes is normally planar up to a medium frequency range (over 1 kHz), and this encourages the use of a combination of reactive and dissipative elements in order to deliver attenuation over a wide frequency range. The reactive elements normally address low frequency noise, especially tonal noise that often arises in power generation, and the dissipative elements address the medium to high frequency range. However, the reactive elements typically consist of resonators placed around the perimeter of the main duct carrying the gas flow, and in order to attenuate sound they depend on the sound pressure field being planar within this duct. This means that once higher order modes begin to cut-on in the main duct the reactive elements no longer work. This is not a problem for smaller systems where higher order modes cut-on in the frequency range where the dissipative element is effective, however this approach presents problems for larger systems where the frequency of the first cut-on mode is much lower. Furthermore, dissipative silencer designs do not work well at low frequencies, and so for larger systems it is possible to have dip in silencer performance in the low to medium frequency range. This presents a classic noise control problem that is well known for larger ductwork.

In larger systems, such as gas turbines, or fans used in heating ventilation and air-conditioning systems, dissipative silencers tend to be used on their own. Moreover, the larger

ductwork means that gas flow velocities reduce to levels that are low enough to enable the silencers to be placed within the main duct. These silencers split the gas flow and the dissipative element again provides good attenuation in the medium to high frequency range. Moreover, splitter silencers can also provide an alternative method for addressing low frequency noise because the act of placing them in the airway delivers reflections from the front and rear baffles. Therefore, in order to address low frequency noise problems using dissipative splitter baffles it is common practice to use large silencers that block an increasing proportion of the duct cross-section in order to deliver higher levels of sound reflection at low frequencies. However, such an approach is clearly unsatisfactory because this will increase the fluid pressure losses over the silencer and so lower the efficiency of the power generating devices, as well as lead to an over-design of the silencer at higher frequencies. Furthermore, standard reactive techniques will not work in the low to medium frequency range because higher order modes will have cut-on in the [larger] ductwork. Accordingly, an alternative approach is required and this article presents ~~a new method for~~ a method for deploying reactive silencer elements in larger ductwork. ~~This aims to~~ that delivers higher levels of sound attenuation in the crucial region between the first cut-on frequency of the main duct, and the frequency at which a typical dissipative splitter silencer begin to perform well.

Power generating devices such as fans and turbines generate tonal as well as broadband noise. Tonal noise is related to the number of blades and speed of rotation of the fan, and Tyler and Sofrin [1] showed that this may be expressed as a sum of spinning modes, which gradually cut-on when they reach a characteristic frequency. Morfey [2] showed that the interaction between the fan blades and non-uniform inlet flow conditions also produces periodic force fluctuations so that broadband noise is generated by the interaction between solid surfaces and an adjacent turbulent flow. This presents a complex noise signature for fans that is made up of a combination of tonal and broad-band components, and it is common

for significant tonal components to appear at low frequencies. It is, of course, attractive to address tonal noise through the use of reactive silencers, as these are capable of delivering high levels of attenuation, although this is restricted to narrow frequency bands.

Accordingly, reactive silencers are very popular noise control techniques and they have been widely studied in the literature, see for example the analysis of multiple resonators by Seo and Kim [3], and more recently by Cai and Mak [4]. These resonators may also be folded to improve low frequency performance [5], or arranged in side branches to encourage coupling between resonator arrays [6]. However, the resonators in these systems are always placed on the perimeter of the main duct and this means they rely on plane wave propagation in the main duct in order to work effectively: beyond the cut-on frequency of the first higher order mode in the main duct, reactive silencers are normally entirely ineffective. This means that for larger ductwork, reactive silencers are generally effective only at very low frequencies and so it is common practice to remove the reactive silencer entirely and to rely on dissipative silencers. Examples of dissipative splitter silencers used in larger systems include the parallel baffle silencers studied by Kirby [7], and Kirby and Lawrie [8], who used analytic and finite element based techniques to obtain the silencer transmission loss over a wide frequency range. This type of silencer has also been analysed using a boundary element approach, see for example Zhou et al. [9] and Wang and Wu [10]. It is common also to use the more complex bar type silencer for larger applications, and these were analysed by Kirby et al. [11], and recently by Yang et al. [12]. The analysis of silencer performance reported in these articles clearly demonstrate that dissipative silencers can be very effective over the medium to high frequency range; however, even the more complex designs find it difficult to deliver acceptable levels of attenuation at low frequency.

In smaller ducts, it is now common to see dissipative and reactive elements combined into a single silencer in order to provide effective levels of noise control over a wide frequency

range. Examples include the hybrid silencer of Selamat et al. [13], and the extended inlets and outlets used by Denia et al. [14], as well as the designs by Lee et al. [15] that were targeted at automotive applications. These hybrid designs continue to use resonators placed on the perimeter of the main duct, and so rely on plane wave propagation for the resonators to be effective; however, they do indicate a potential way forward to addressing noise control in much larger ductwork. ~~Furthermore~~For example, this strategy has recently been applied to larger power generating systems Papini et al. [16], who introduce a hybrid reactive-dissipative that uses up to three different resonators designed to operate up to a frequency of 250 Hz. However, ~~it appears that~~ Papini et al. continue to apply the reactive elements in the traditional way, so that resonators are placed on the duct perimeter only and the reactive elements continue to rely on plane wave propagation in the main duct. Moreover, the authors do not report measurements or predictions of hybrid silencer performance over a broad frequency range, and so it is difficult to fully evaluate the success of their approach. However, it is clear that there is a need to draw on the well-established principles behind the use of a hybrid dissipative-reactive approach, and to apply these in larger systems in such a way that effective levels of attenuation are provided over a wide frequency range. One possible approach is to incorporate reactive elements into the splitter baffles themselves rather than placing them around the perimeter of the duct. ~~Crucially~~For example, if one places these hybrid splitter baffles along the nodal lines of higher order modes propagating inside the main duct, then it ~~appears to be~~is possible to partition up the duct so that each reactive element effectively experiences close to planar type pressure distributions over their individual section of the [partitioned] duct. Whilst the sound pressure distribution will not be planar when higher order modes propagate, it is likely to be close to planar over sections of the duct in a limited frequency range above the first cut-on frequency. This offers the potential to extend reactive silencer performance above the first cut-on mode in the main

duct, and through careful partitioning of the duct and alignment of baffles, ~~it appears to be this~~ will enable possible to target particular higher order modes to be targeted using different silencer designs. For example, a bar silencer [11, 12] may target different higher modes when compared to a parallel baffle type silencer [7]. Of course, each resonator will continue also to provide good sound attenuation below the first cut-on mode of the main duct. Accordingly, this approach offers the potential for reactive elements to cover provide attenuation over a wider frequency range than is normally found when they are placed on the duct walls.~~so that the reactive elements address the low to medium frequency range, and the dissipative elements are required only to address the medium to high frequency range.~~ This has the potential to reduce the size of the ~~then enables the~~ dissipative silencer because it is no longer the only means of providing attenuation at low~~to be sized correctly, and for the blockage area of the silencer to be optimised so that the pressure losses from the fluid flow are minimised for a particular application~~ frequencies. Accordingly, the fundamental principles behind this new hybrid silencer design are discussed further in the following section. A theoretical model then follows in section 3 to enable the optimisation of silencer design and to investigate the robustness of the design. Silencer performance is then measured in the laboratory and this is reported section 4, with discussions and conclusions following in sections 5 and 6.

## **2. Hybrid Silencer Design**

Combining the acoustic performance of reactive and dissipative silencer elements is best achieved for large ductwork by combining the two elements together in each baffle. This approach also has practical advantages, because this configuration is easier to manufacture, install and maintain. Moreover, fabricating two separate (dissipative and reactive) units is



likely to be more expensive, and separating these units may also lead to higher fluid pressure drops due to increased turbulence in the flow. Accordingly, the hybrid silencer element proposed here consists of a section of dissipative silencer attached to a reactive resonant chamber. Three different possible designs are illustrated in Fig. 1, where a simple dissipative baffle is joined to simple resonant chamber designs. The front of the hybrid baffle design consists of a bullnose fairing that smooths the mean gas flow past the baffle. Behind this, a dissipative section is added so that the resonant chamber is placed at the rear of the baffle. The first resonator is a simple empty chamber, whereas the second and the third designs contain partitions, and the reasons behind this will be discussed in sections 4 and 5.

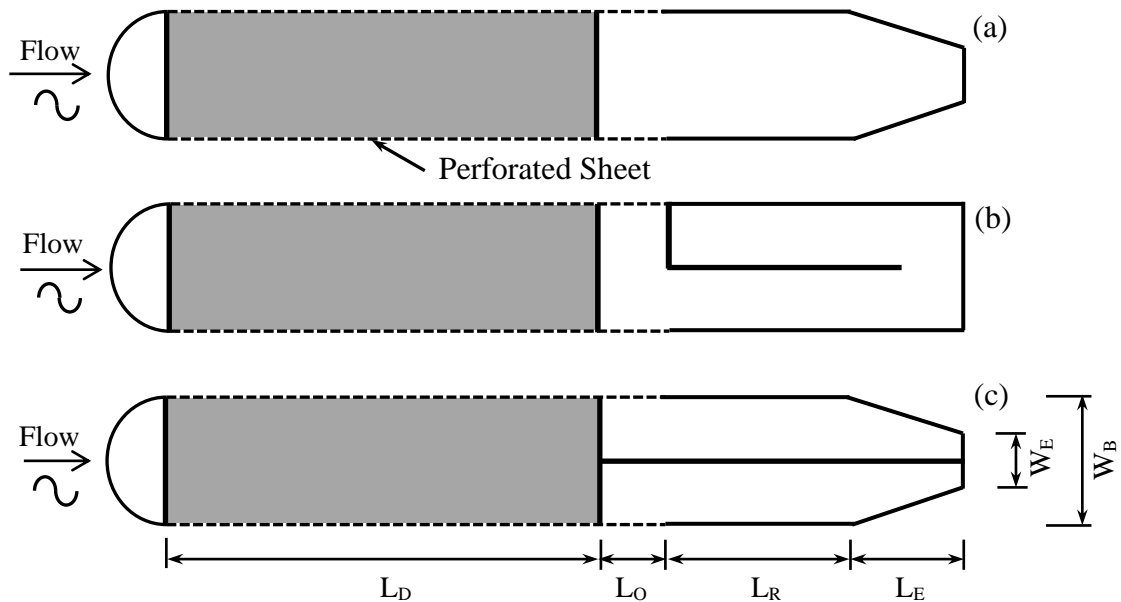


Figure 1. Geometry of a hybrid baffle. (a) Type 1 resonator; (b) Type 2 resonator; (c) Type 3 resonator

The frequency at which a resonator is most effective is of course dictated by the length of the resonator, however resonator design must also take into account the size of the resonator opening because this dictates the width of the resonant peak. This means that larger resonator opening areas are more effective up to the limit of the area of the opening equalling that of the resonator, beyond which there is nothing to be gained from increasing the open area. Therefore, it is desirable to try and maximise the size of the resonator opening in Fig. 1,

although this is at the expense of a reduction in the resonator length, and so this alters the frequency at which the resonator is effective. Accordingly, one must achieve a balance between the area of the opening and the length of the resonator, and this is achieved here by the use of computational models described in the next section. Note that each resonator opening also contains a perforated sheet aligned in parallel with the mean flow in order to smooth the gas flow over the opening. The perforated sheet is also designed to eliminate whistling at the throat of the resonator when a mean gas flow is present – whistling may be induced by vortex shedding in the mean gas flow as it moves over the backward facing step that would be present if the perforated sheet was omitted. The acoustic impedance of this perforated sheet will also influence the acoustic performance of the resonator, however provided perforation porosities above 20% are used, the perforated sheet is not expected to have a significant effect on the acoustic characteristics of the resonator.

The underlying principle of the designs in Fig. 1 is that a number of these reactive sections are placed in parallel within the main duct, so that they form part of the usual splitter silencer arrangement, which is shown in Fig. 2 for a parallel baffle design. In Fig. 2, two parallel splitters ( $n_b = 2$ ) are shown, although as the size of the duct increases it is common to add more baffles, rather than the alternative of fixing the baffle number and then increasing the width of each baffle. The practice of increasing baffle number is, therefore, advantageous for the proposed hybrid design because the reactive elements are to be located at regular intervals across the width of the duct. This will enable the targeting of nodal pressure lines in higher order modes and for the method to continue to be applicable when larger ductwork is encountered. Of course, this further adds to the complexity of a hybrid silencer design and it is clearly possible to design many different configurations for the baffles and dissipative/reactive elements, and to use many different parameters for the porous materials and the perforated sheets. Accordingly, the resonators chosen in Fig. 1 have been designed

with simplicity in mind in order to facilitate a basic investigation into a new hybrid design that can also be readily manufactured with minimal additional costs. Moreover, only a single hybrid baffle design is used in each test silencer, so that  $n_b$  baffles based on one reactive design from Fig. 1(a), 1(b), or 1(c), is used rather than mixing different designs. It is of course possible to design more complex resonator/dissipative element combinations, however it is thought that more complex designs are likely only to deliver marginal gains in performance and also incur extra fabrication costs. Furthermore, even relatively simple hybrid resonator designs contain a large number of variables that need to be identified and optimised before fabrication. Resonators also normally work only in relatively narrow frequency bands, and so one must be very careful to design for both the appropriate resonant frequency but also the width of the resonant peak. It is important therefore to build sufficient contingency into the design in order to successfully attenuate a given tonal noise problem which may not be at exactly the frequency expected. This means that the only feasible approach to optimising the design of this type of hybrid silencer is to use a computational model to engage in an interactive design procedure. Accordingly, this computational model is discussed in the next section.

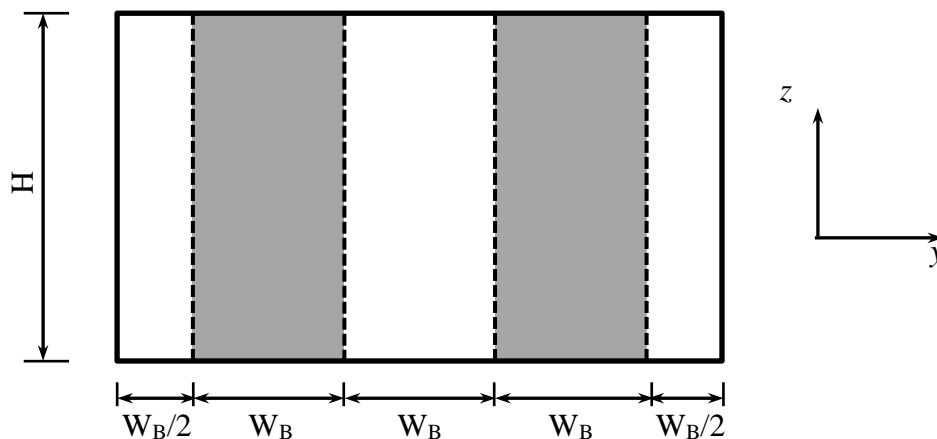


Figure 2. Geometry of cross-section of silencer with two baffles ( $n_b = 2$ ).

### 3. Theory

The analysis of a hybrid silencer design is best achieved using a numerically efficient approach that makes use of modal expansions in the inlet and outlet (empty) duct sections, and then joins this to a full finite element based discretisation of the reactive/dissipative silencer section. This delivers a reasonably efficient computational approach, although it is noted that further efficiency savings could be achieved by taking advantage of any regions of uniformity within the silencer section itself. However, in order to facilitate flexibility when it comes to investigating different designs, a full finite element discretisation is used here for the silencer region. The silencer geometry is shown in Fig. 3, and here a two-dimensional

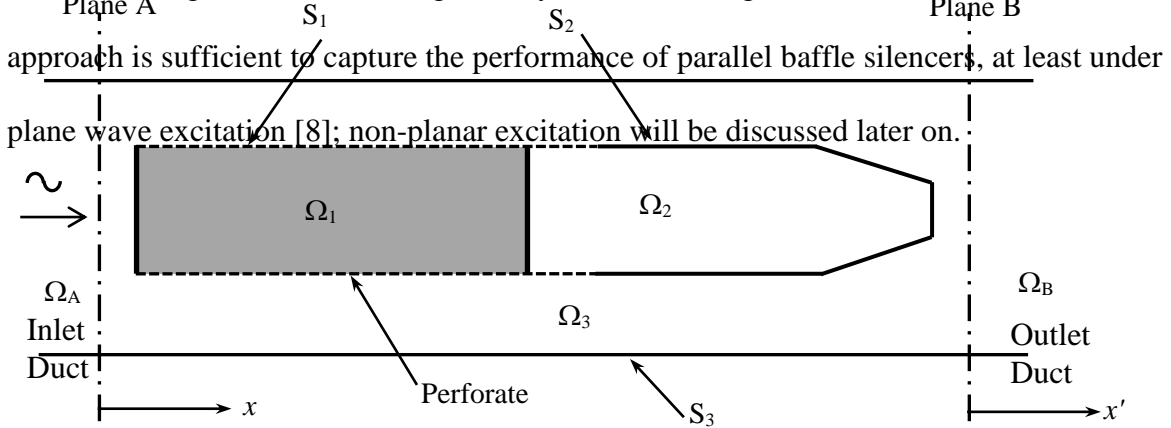


Figure 3. Geometry of hybrid silencer.

In Fig. 3 sound travels down a uniform inlet duct, region  $\Omega_A$ , and is incident on the silencer at the vertical plane A, where  $x = 0$ . Note that it is sufficient here to assume that the bull-nose fairing at the front of the silencer is flat, as the curvature has little influence on sound propagation [17]. The silencer section has an overall length  $L = L_D + L_O + L_R + L_E$ , and consists of a dissipative element, region  $\Omega_1$ , a reactive element, region  $\Omega_2$ , and a

surrounding empty section, region  $\Omega_3$ . Plane B is placed at the other end of the silencer, at  $x' = 0$ . Every surface in the silencer is assumed to be an acoustically hard wall apart from the perforated screens, which appear in Fig. 3 as dashed lines. Further, the outer surface of region  $\Omega_1$  is denoted  $S_1$ , and so on.

The theoretical analysis that follows makes use of the numerical method reported by Kirby [18] for automotive silencers, and later by Kirby et al. [17] for splitter silencers similar to those studied here. Therefore, this method will not be discussed in great detail here, so that only the key equations and boundary conditions are reported. Accordingly, in the absence of mean flow, the governing wave equation for sound propagation in any region  $q$ , is given as

$$\frac{1}{c_q^2} \frac{\partial^2 p_q}{\partial t^2} - \nabla^2 p_q = 0 \quad (1)$$

where,  $c$  is the speed of sound and  $p$  is the acoustic pressure in region  $q$ , and  $t$  is time. A time dependency of  $e^{i\omega t}$  is assumed throughout this article, where  $i = \sqrt{-1}$  and  $\omega$  is the radian frequency. In addition, the terminology  $k_0 = \omega/c_0$  will be used, where the subscript zero refers to the wavenumber and speed of sound in air, which applies to all regions except the porous material,  $\Omega_1$ . The modelling approach uses a modal expansion for regions  $\Omega_A$  and  $\Omega_B$ , and for two-dimensions this yields

$$p_A(x, y) = \sum_{m=0}^{\infty} A_m \Psi_m(y) e^{-ik_0 \lambda_m x} + \sum_{m=0}^{\infty} B_m \Psi_m(y) e^{ik_0 \lambda_m x} \quad (2)$$

$$p_B(x', y) = \sum_{m=0}^{\infty} C_m \Psi_m(y) e^{-ik_0 \lambda_m x'} \quad (3)$$

where  $A_m$ ,  $B_m$  and  $C_m$  are modal amplitudes, and  $\lambda_m$  are the eigenvalues and  $\Psi_m$  the eigenvectors for ducts  $\Omega_A$  and  $\Omega_B$ , assuming the ducts are identical. Equation (3) also assumes that there are no reflections in the outlet duct. To obtain the eigenvalues and

eigenvectors, the expansions in Eqs. (2) and (3) are substituted back into the wave equation to create an eigenproblem that is solved using finite elements [7, 18]. This requires the substitution of the zero normal particle velocity boundary condition over each hard wall, and this is then solved using the “eig” function in MATLAB®.

In the central section, between planes A and B, a full finite element solution is adopted. This involves discretising the sound pressure inside each region, so that for region  $q$ , where  $q = 1, 2$  or  $3$ ,

$$p_q(x, y) = \sum_{j=1}^{M_q} N_{qj}(x, y) p_{qj}, \quad (4)$$

where  $N_q$  is a global shape function for the finite element mesh, and  $p_q$  is the value of the acoustic pressure at node  $j$ . The total number of nodes (or degrees of freedom) in region  $\Omega_q$  is then  $M_q$ , and the total number of nodes in the finite element mesh is  $M_T = M_1 + M_2 + M_3$ . Equation (4) may be expressed in vector form, so that  $p_q = \mathbf{N}_q \mathbf{p}_q$ , where  $\mathbf{N}$  is a row vector and  $\mathbf{p}$  is a column vector, each of length  $M_T$ . Following previous investigations [7, 17], a weighted residual statement for the governing wave equation yields

$$\left[ \int_{\Omega_q} [\nabla \mathbf{N}_q^T \nabla \mathbf{N}_q - k_q^2 \mathbf{N}_q^T \mathbf{N}_q] dx dy \right] \mathbf{p}_q = \int_{S_q} \mathbf{N}_q^T \nabla p_q \cdot \mathbf{n}_q dS_q \quad (5)$$

where  $k_2 = k_3 = k_0$ , and  $k_1 = -i\Gamma$ , with  $\Gamma$  the propagation constant for the porous material [18]. In addition,  $S_q$  denotes the outer surface of region  $\Omega_q$ , and  $\mathbf{n}_q$  is a unit normal pointing outwards from  $\Omega_q$ . When the outer surface of region  $\Omega_q$  is a hard wall, then the boundary condition of zero normal particle velocity means that the right hand side of Eq. (5) is zero. However, if the outer surface is a perforated sheet, then continuity of normal particle velocity is enforced across the sheet, as well as the following pressure condition:

$$p_3 - p_{1,2} = \rho_0 c_0 \zeta \mathbf{u}_3 \cdot \mathbf{n}_3 \quad (6)$$

Here, it is assumed that the perforated screen is placed between region  $\Omega_3$  and either regions  $\Omega_1$  or  $\Omega_2$ . Further,  $\rho_0$  is the fluid density in air,  $\zeta$  is the (dimensionless) impedance of the perforated screen, and  $\mathbf{u}_3$  is the velocity in region 3. Substitution of this boundary condition into Eq. (5), and adding together each region yields,

$$\mathbf{G}\mathbf{p} - \mathbf{Q}_A^T \mathbf{B} + \mathbf{Q}_B^T \mathbf{C} = \mathbf{Q}_A^T \tilde{\mathbf{A}} \quad (7)$$

The matrices in Eq. (7) are given in Appendix A. In addition,  $\tilde{A}_m = A_m e^{-ik_0 \lambda_m (x - x_s)}$ , where  $x_s$  is the location of the source in duct  $\Omega_A$ , which is relevant only when higher order modes are incident upon the silencer, see later analysis. The modal amplitudes have been written in vector form, so that  $\tilde{\mathbf{A}}$  is a column vector, and so on. Two further sets of equations are required in order to solve the problem, and these are continuity of pressure over planes A and B, which yields

$$\mathbf{M}_A \tilde{\mathbf{A}} + \mathbf{M}_A \mathbf{B} - \mathbf{Q}_A \mathbf{p}_{3A} = 0 \quad (8)$$

and

$$\mathbf{M}_B \mathbf{C} - \mathbf{Q}_B \mathbf{p}_{3B} = 0, \quad (9)$$

where  $\mathbf{p}_{3A,B}$  is a column vector holding the nodal values of pressure on planes A or B, and matrices  $\mathbf{M}_A$  and  $\mathbf{M}_B$  are given in the appendix. Finally, Eqs. (7), (8) and (9) are combined to give the final system matrix:

$$\begin{bmatrix} \mathbf{M}_A & -\mathbf{Q}_A & \mathbf{0} & \mathbf{0} & \mathbf{0} \\ -\mathbf{Q}_A^T & \mathbf{G}_{AA} & \mathbf{G}_{AS} & \mathbf{G}_{AB} & \mathbf{0} \\ \mathbf{0} & \mathbf{G}_{SA} & \mathbf{G}_{SS} & \mathbf{G}_{SB} & \mathbf{0} \\ \mathbf{0} & \mathbf{G}_{BA} & \mathbf{G}_{BS} & \mathbf{G}_{BB} & \mathbf{Q}_B^T \\ \mathbf{0} & \mathbf{0} & \mathbf{0} & \mathbf{Q}_B & -\mathbf{M}_B \end{bmatrix} \begin{pmatrix} \mathbf{B} \\ \mathbf{p}_{3A} \\ \mathbf{p}_S \\ \mathbf{p}_{3B} \\ \mathbf{C} \end{pmatrix} = \begin{pmatrix} -\mathbf{M}_A \tilde{\mathbf{A}} \\ \mathbf{Q}_A^T \tilde{\mathbf{A}} \\ \mathbf{0} \\ \mathbf{0} \\ \mathbf{0} \end{pmatrix}, \quad (10)$$

where  $\mathbf{P}_S$  is a column vector that holds the pressures at the nodes in regions  $\Omega_1$ ,  $\Omega_2$ , and  $\Omega_3$ , that do not lie on planes A and B, whereas  $\mathbf{P}_{3A}$  and  $\mathbf{P}_{3B}$  hold the values that do lie on planes A and B, respectively.

To solve Eq. (10) it is necessary to assign properties for the incident sound field and in this article two different sound fields are used: a plane wave, so that  $A_0 = 1$ , and  $A_m = 0$  for  $m > 1$ ; and equal modal energy density (EMED), see Mechel [19], which gives [17]:

$$\left| \frac{A_j}{p_0} \right|^2 = \frac{I_0}{I_j \sum_{m=0}^{M_A} \lambda_m}, \quad (11)$$

where,  $M_A$  is the number of modes found on solution of the eigenproblem in region  $\Omega_A$ , and  $I_j = \int |\Psi_j(y)|^2 dy$ . The silencer transmission loss, TL, is then defined as the ratio of the inlet to the outlet sound power, and so in general this gives:

$$TL = -10 \log_{10} \sum_{m=0}^{M_A} \frac{\text{Re}(\lambda_m) I_m |C_m|^2}{I_0}. \quad (12)$$

#### 4. Experiment

To validate the new hybrid silencer designs, experimental data is obtained using a test rig designed to measure silencer insertion loss (IL). Silencer IL is normally obtained by measuring the attenuation of a silencer in a duct, and then comparing this with an identical set of measurements obtained for the same duct but with the silencer removed. This approach aims to deliver values of IL that are, as far as possible, equivalent to the TL values obtained using theoretical models in the previous section. However, some inaccuracies inevitably arise from this approach, and the most important of these are thought to be related to the change in source impedance between measurements undertaken with and without the silencer present, see for example the discussion on this subject by Kirby et al. [17]. Nevertheless,



comparisons between predicted TL and measured IL have been shown to be sufficiently good to provide meaningful information [11, 12], especially in the lower to medium frequency range, which is of most interest in this article. Accordingly, the IL of the parallel baffle designs described in section II are measured here, and this is accomplished using a test duct that runs from an anechoic chamber to a reverberation room, see Fig. 4.

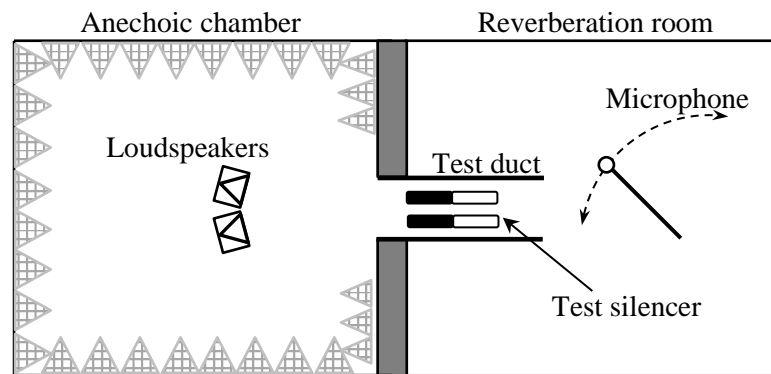


Figure 4. Experimental facility for measuring silencer insertion loss.

The test duct is 800 mm wide and 600 mm high, and it is made from steel panels 1.5 mm thick. This means that the cut-on frequencies for the first four higher order modes in the large 800 mm direction are:  $f_1 = 214$  Hz,  $f_2 = 428$  Hz,  $f_3 = 642$  Hz,  $f_4 = 856$  Hz. . The duct is 1835 mm long and it is attached to the wall that separates the anechoic chamber from the reverberation room. Five loudspeakers are arranged so that two of them sit on top of the other three. The distance between the loudspeakers and the entrance to the test duct is approximately 1500 mm. The loudspeakers are Cerwin-Vega VS Series, and they are driven in phase using B&K pulse software to generate white noise fed through Zachary type XP-250 power amplifiers. The reverberation room is used as the receiving room and this room is used to measure the sound power at the exit from the ductwork, before and after the addition of the test silencer. Sound power is measured in the reverberation room using a remotely controlled rotating boom. The boom is B&K type 3923, and this supports a BSWA MP201

microphone, which is fed into a BSWA MA201 microphone pre-amplifier; data is captured and averaged using B&K Pulse software. The sound power is calculated following a continuous sweep of the boom, which is calibrated to measure at a sufficient number of locations in order to accurately determine the sound power radiated by the duct. The sweep takes approximately 32 seconds to complete, and the sound power is calculated in one-third octave bands. Thus, the measured values for IL reported in the following section cover a centre frequency range from 50 Hz to 8 kHz in one third octave bands. The repeatability of the measured IL values was examined by undertaking 10 IL measurements on following the removal and re-insertion of silencer 1. A mean average of these measurements was then taken for silencer 1 and errors bars that represent two standard deviations from the mean were calculated. In view of the time it takes to obtaining these error bars, the repeatability of the values obtained for silencer 1 are assumed also to apply to the other measurements reported in this article.

The test facility is suitable for measuring the IL of relatively small splitter silencers and this is reflected in the geometries chosen for each test. However, before undertaking these tests it is important first to measure the limiting IL for the test rig. This was obtained by measuring the IL of the test duct blocked with four thick wooden panels that were glued together and then backed by a dense fibrous material. The limiting IL values obtained are included in the plots that follow, in order to indicate where the performance of the silencer is beginning to approach the limits of the test facility. The investigation that follows is aimed at examining the influence of the reactive element, and so a standard dissipative section is used for each silencer configuration, and the reactive section is then changed for each test. This delivers six different configurations and these are number individually and listed in Table 1.

Table 1. Dimensions for test silencers. [Please complete]

Silencer	$n_b$	$L_D$ (mm)	$L_O$ (mm)	$L_R$ (mm)	$L_E$ (mm)	$W_B$ (mm)	$W_E$ (mm)	Type	Target Frequency
1	2	900	-	-	-	200	-	-	-
2	2	900	<u>100</u>	<u>365</u>	<u>300</u>	200	<u>121</u>	1	125
3	2	900	<u>100</u>	<u>20</u>	<u>300</u>	200	<u>121</u>	1	250
4	2	900	<u>100</u>	<u>20</u>	<u>70</u> <u>read</u> <u>note</u> <u>below</u>	200	<u>121</u>	1	500
5	2	900	<u>50</u>	<u>215</u>	-	200	-	2	175
6	2	900	<u>50</u>	<u>140</u>	-	200	-	2	250
7	<u>2</u>	<u>900</u>	<u>100</u>	<u>365</u>	<u>300</u>	200	<u>121</u>	3	<u>125</u>

[Please complete as you see fit, so that you are happy with the amount of data you are relasing, but making sure the dimensions do make some sort of sense]

The dissipative element is made using rock wool, which has a flow resistivity of 21,400  $\text{kgs}^{-1}\text{m}^{-3}$ , and this was measured according to ISO 29053 [20]. The acoustic properties of the rock wool are the same as in the previous study by Kirby et al. [11], so that

$$\Gamma/k_0 = 0.2722\xi^{-0.4718} + i[1 + 0.2432\xi^{-0.4326}] \quad (13)$$

and

$$\rho_1 = -\rho_0(\Gamma/k_0)\{0.1591\xi^{-0.5328} + i[1 + 0.1316\xi^{-0.5391}]\}. \quad (14)$$

Kirby [21] shows why these values are not valid at low frequencies, and so the low frequency corrections described by Kirby and Cummings [22] are used here, with a value of 2.48 for the steady flow tortuosity and a transition value of  $\xi = 0.011$ . Finally, the data for the perforated screen use the expressions reported in a number of articles by the authors, see

for example Kirby et al. [11], where the properties of air are substituted for those of the porous material when calculating the impedance in the reactive section. The thickness of the perforated screen is 1.6 mm, the hole diameter is 3 mm, and the porosity is 27%.

## 5. Results and Discussion

To validate the hybrid silencer concept, comparisons are made in this section between predicted TL and measured IL for a number of different hybrid silencer designs. TL is the difference between the incident and transmitted sound powers, whereas IL is the difference between the sound power with and without a silencer installed. It is assumed in the comparisons that follow that TL and IL are equivalent, which will be true if the sound power incident upon the test duct during the experiment remains the same with and without the silencer installed. In practice, there is likely to be some change in the incident sound power, and this will be seen as local oscillations in the IL curves; however, this effect is seen to be negligible in the measured data that follows, especially once this data has been averaged into one-third octave bands.

However, it is sensible to start by comparing prediction and measurement for a dissipative element on its own, as this enables comparison with previous studies on dissipative splitter silencers [11, 17]. Accordingly, in Figure 5, the IL measured using the methodology described in the previous section is compared against predictions for silencer 1, which is a dissipative splitter on its own, see also Table 1. Silencer 1 has two parallel dissipative baffles and it is excited by a plane wave in the theoretical model, which means that one can take advantage of symmetry in order to model only a single baffle. However, even when using this approach, to obtain a converged solution at the highest frequency for this type of dissipative silencer it is still necessary to employ 318,097 finite element nodes in the central section, as well as 161 modes in the inlet duct and 273 modes in the outlet duct.

This delivers a final system matrix (Eq. (10)) of order 318,531, which took 87 seconds to solve for a single frequency, although it is possible to reduce this to an average of 8.3 seconds per frequency, when studying multiple frequencies.

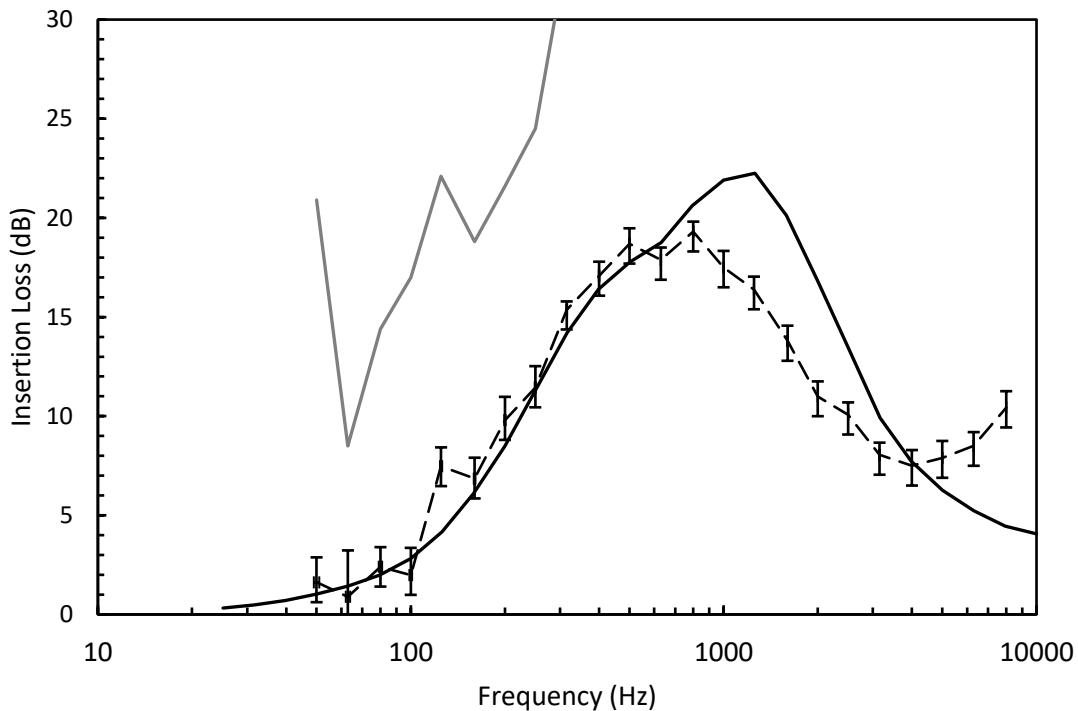


Figure 5. Comparison between measured and predicted IL for a dissipative element on its own (Silencer 1). —, prediction; - - - , measurement; —, limiting IL.

A comparison between prediction and measurement in Fig. 5 shows a level of agreement similar to that seen for dissipative baffles in previous studies [11, 12, 17]. At low to medium frequencies the agreement is generally good, although at higher frequencies an over-prediction similar to that seen in other studies is also found here. This over-prediction is well-known, although the reasons behind this are not yet fully understood. However, this does not unduly effect this current study, as the focus here is on the influence of the reactive elements and this is limited to the low to medium frequency range where agreement between prediction and measurement is generally good. Note that Fig. 5 also reveals two issues with the experimental test facility: (i) at low frequencies a small peak in the IL is observed at 125 Hz, and this is thought to be caused by an axial resonance in the test duct; and, (ii) at high

frequencies the measured data flattens out, which does not reflect the expected performance of this type of silencer, especially if one compares this to the consistent reduction in the IL seen in previous studies [11, 17]. Nevertheless, the agreement between prediction and experiment is sufficiently good over the frequency range of interest to provide confidence in the validation of a hybrid baffle that follows.

A hybrid baffle design is obtained by adding different reactive element designs onto the same dissipative section. Three different reactive designs are studied here, which are labelled types 1 to 3 in Fig. 1. Each reactive element can be tuned to a different fundamental resonance frequency, which is accomplished by changing the length and/or the design of the reactive element. This makes up six different hybrid silencer designs, and these are labelled silencers 2 to 7 in Table 1, which also includes the respective geometry of each silencer. Silencer 2 consists of a type 1 reactive element added on to the back of silencer 1, which has been tuned to a fundamental resonant frequency of 125 Hz. A comparison between the IL measured with and without the reactive element is shown in Fig. 6. This figure also includes theoretical predictions for silencer 2, which requires the modelling of the additional reactive element and this increases the degrees of freedom required in the central section to 364,042. It is immediately apparent in Fig. 6 that the addition of a resonant chamber delivers the expected increase in IL at the design frequency of 125 Hz. The measured increase is approximately 10 dB, although this large increase in performance at a relatively low frequency means that the silencer IL is now close to the limiting IL of the test rig, and so some caution should be exercised here when quantifying this increase. However, this rise in IL is consistent with predictions, which also identify a strong peak at 125 Hz. Moreover, agreement between prediction and measurement is generally seen to be good over the low to medium frequency range and this is at least comparable to that seen in Figure 5, provided one

remembers that the model does not include structural damping in the chamber walls so that some over-prediction at resonance is to be expected.

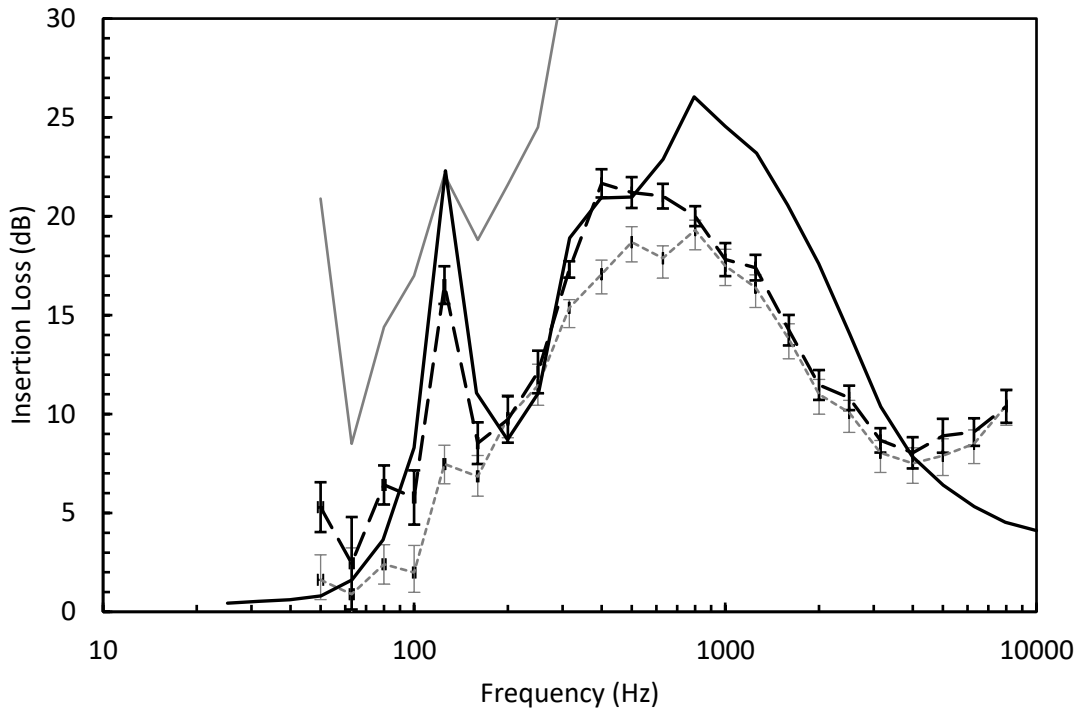


Figure 6. Comparison between measured and predicted IL for new type 1 hybrid design, with target frequency of 125 Hz. ———, predictions for silencer 2; - - - - measurement for silencer 2; ······ measurement for silencer 1; ———, limiting IL.

It is interesting to observe in Fig. 6 that the first resonance peak extends to the width of a 1/3 octave band, so that additional levels of attenuation are achieved from 100 Hz to 160 Hz. This is important because the width of the resonant peak allows one to build some contingency into the design of the silencer, so that for real applications small changes in the tonal frequencies of the sound source can be accommodated. Figure 6 also reveals that additional attenuation is obtained at frequencies beyond the original target frequency of 125 Hz. For example, an increase of approximately 5 dB is also observed at 400 Hz, and again this increase extends to at least a 1/3 octave band. Furthermore, this increase in IL is observed at frequencies above the first two cut-on modes of the test duct (y direction), which occur at 214 and 428 Hz. This increase in performance at higher frequencies is caused by

resonance at odd multiples of the fundamental resonance frequency and demonstrates that, through the appropriate placement of reactive silencer elements inside the duct, it is possible to obtain additional attenuation from reactive elements outside of what is normally considered to be their working frequency range.

To further explore the behaviour seen in Fig. 6, the target frequency of the reactive element is changed to 250 Hz in Fig. 7, and 500 Hz in Fig. 8. For these two designs, the same dissipative element is used (from silencer 1) and the reactive chamber design continues to be type 1. However, to deliver different fundamental resonance frequencies, the length of the reactive chambers is lowered to produce two new silencer designs: silencer 3 (Fig. 7) and silencer 4 (Fig. 8), see Table I for respective geometries. Note that the theoretical predictions have been removed from these figures in order to aid in the comparison between designs. It can be seen in Figs. 7 and 8 that very similar behaviour is obtained when adding the new resonance chambers, so that for silencer 3 an increase of approximately 8 dB is observed at 250 Hz, and a further increase of about 5 dB is seen at 630 Hz. Figure 7 again illustrates that additional attenuation from the reactive chamber may be obtained over a relatively wide frequency range. Furthermore, the target frequency of 250 Hz is above the first cut-on of the main duct, and Fig. 7 shows that the resonant chamber continues to work outside the plane wave region of the main duct. This behaviour is also observed for a target frequency that is above two higher order modal cut-on frequencies, so that in Fig. 8 a target frequency of 500 Hz delivers an increase in IL of approximately 7 dB.



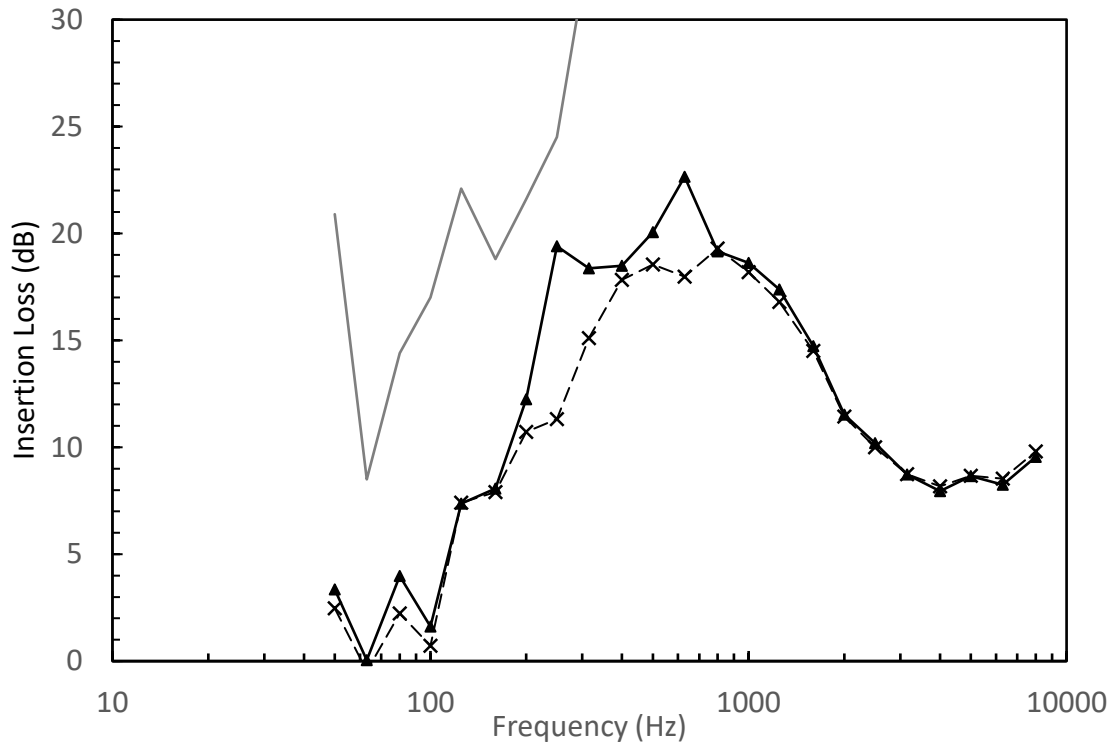


Figure 7. Measured IL for type 1 hybrid design with target frequency of 250 Hz.

—▲—, hybrid silencer 3; - - - x - - -, dissipative silencer on its own (silencer 1);  
 —, limiting IL.

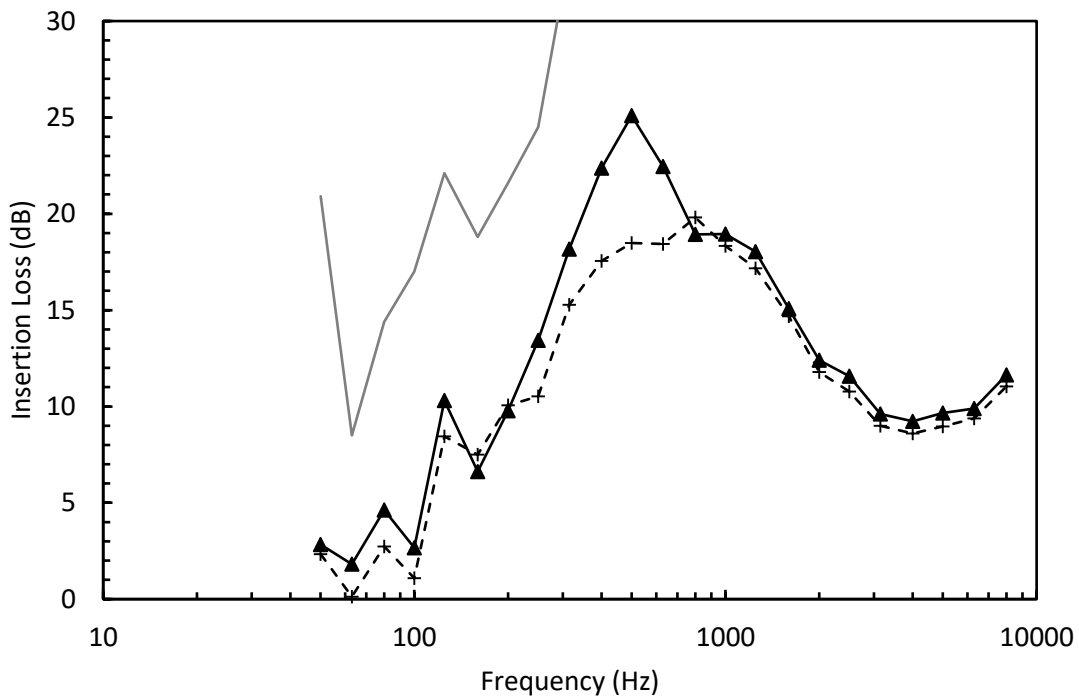


Figure 8. Measured IL for new type 1 hybrid design with target frequency of 500 Hz.

—▲—, hybrid silencer 4; - - - x - - -, dissipative silencer on its own (silencer 1)  
 ; —, limiting IL.

Thus, it is seen in Figs. 6-8 that not only can a reactive element deliver an increase in IL at harmonics that are above the first cut-on frequency, it can also deliver attenuation when the fundamental resonant frequency is above the first or second cut-on. However, once one passes the fourth cut-on frequency then the reactive component starts to become inactive, so that in Fig. 8 it is seen that the multiple resonant behaviour of silencers 2 and 3 no longer appear because the frequency is too high to support this. However, the results presented here indicate that it may be possible to address this by adding additional splitter sections.

A key problem with tonal noise is achieving sufficient levels of attenuation at low frequencies. The type 2 chamber in Fig. 1(b) is designed to target lower frequencies by increasing the effective length of the resonant chamber. Of course, this is at the expense of lowering the open area of the chamber, and so the frequency bandwidth over which the chamber is active will reduce. However, it is interesting to review here the performance of this type of design as it is likely to be an important tool in addressing very low frequencies. Accordingly, in Fig. 9 a type 2 chamber is tuned to 175 Hz, and in Fig. 10 the same chamber is tuned to 250 Hz. These new chamber designs are added to the dissipative component of silencer 1 in the same way as before, to form two new designs, silencers 6 and 7, respectively, see Table I. The performance of these hybrid designs are also compared against silencer 1, and theoretical predictions are again omitted for clarity. It is seen in Figs. 9 and 10 that this type of chamber is also capable of delivering increases in IL that are similar to those seen for a type 1 design. That is, a significant increase in IL is observed at the design frequency, whilst increases are also seen at higher multiples of the fundamental frequency. However, it is evident for a type 2 design that the increase in IL at higher frequencies does not reach the levels seen for the type 1 chamber, and the design is less effective above 500 Hz because of the narrower width of the chamber. This illustrates some of the limitations of this

approach, and also the importance of carefully designing this type of silencer first before one can expect to realise the anticipated gains in performance.

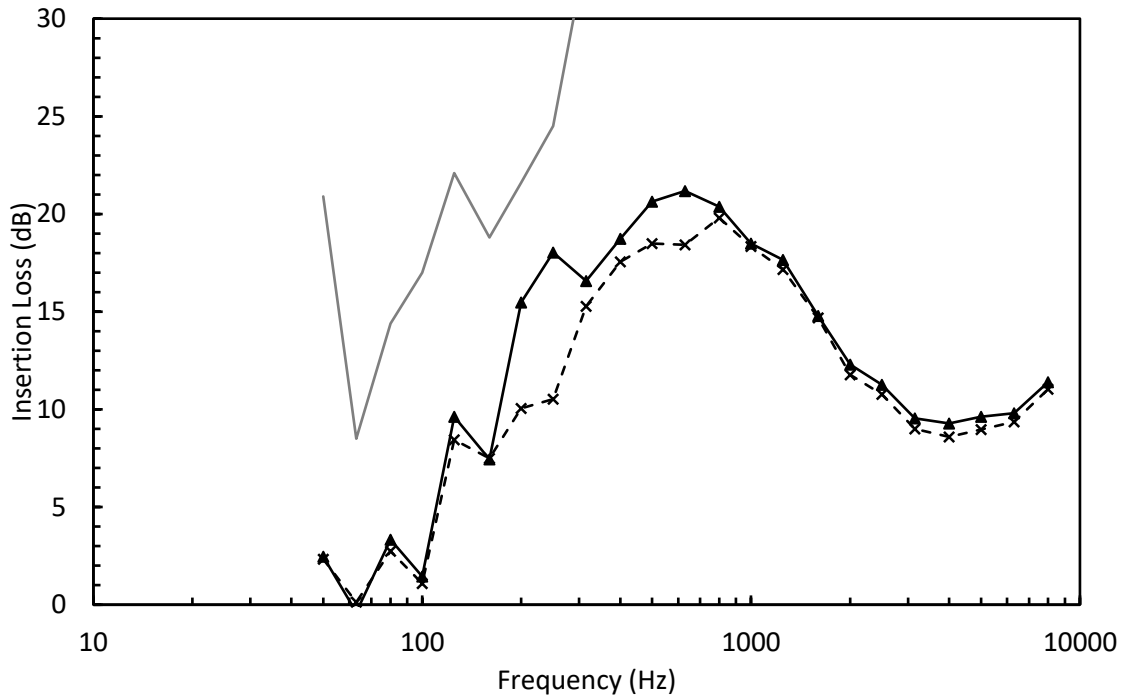


Figure 9. Measured IL for new type 2 hybrid design with target frequency of 175 Hz.

—, hybrid silencer 5; - - - -, dissipative silencer on its own (silencer 1);  
; —, limiting IL.

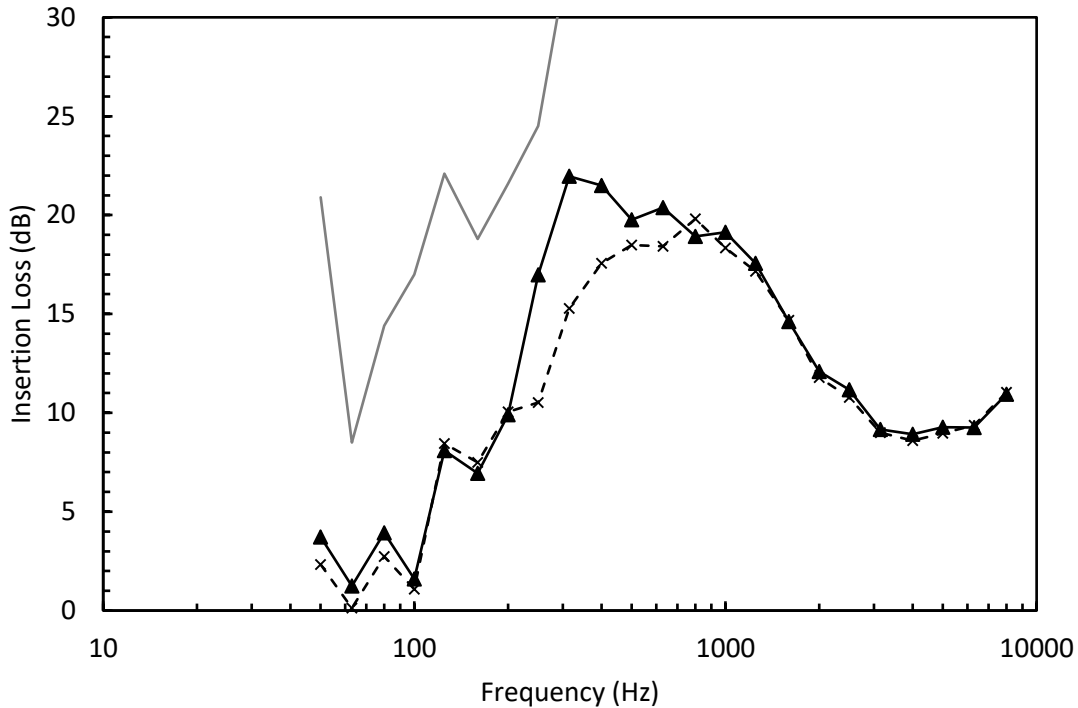


Figure 10. Measured IL for new type 2 hybrid design with target frequency of 250 Hz.

———, hybrid silencer 6; - - - - -, dissipative silencer on its own (silencer 1);  
 ———, limiting IL.

The results presented in Figs. 6-10 demonstrate the action of the hybrid dissipative-reactive baffle design, and demonstrate that it can work successfully under laboratory conditions. However, reactive elements tend to be more sensitive to inlet conditions when compared to dissipative elements, and so reactive systems need to be designed to account for conditions one may find in practice rather than under controlled laboratory conditions. One potential area of concern is the performance of reactive elements when they are exposed to non-planar incident sound fields. Turbomachinery is known to generate non-planar sound fields, see for example Tyler and Sofrin [1], or Mechel [19], and it is possible that non-planar incident waves will remove the behaviour seen here at frequencies above the first cut-on. The influence of non-planar excitation has been considered before for dissipative splitter silencers, see for example Kirby and Lawrie [8], and in their article they used the equal modal energy density (EMED) excitation reported by Mechel [19], as this was thought to be the most appropriate representation for turbomachinery noise. Accordingly, the performance of a

hybrid silencer is investigated here for plane wave and EMED excitation using the theoretical model described in section 4, with the EMED sound source placed 7 m from the front end of the silencer. In Fig. 11, the predicted TL for silencer 2 is presented for both plane wave and EMED excitation and it is evident that when one moves above the cut-on frequency of the first higher order mode in the main duct, that EMED excitation begins to lower the IL seen previously for plane wave excitation. This is most obvious above the second cut-on frequency where the performance of the silencer under EMED begins to drop significantly. This illustrates how important the properties of the incident sound field are on the performance of a reactive component, and illustrate that this silencer must be carefully designed. The reason for this loss of performance at higher frequencies is that the incident energy is now propagating at different angles to the silencer axis, and the transverse sound pressure field within the silencer begins to depart more quickly from the quasi-planar profile that supported the reactive silencer performance under plane wave conditions. In order to restore performance, it is necessary to further partition the duct and this is achieved by placing a central partition in the type 1 design to form the type 3 chamber design shown in Fig. 1(c). The predicted performance of a type 3 hybrid design is also included in Fig. 11, and it is clear that partitioning up the chamber has now restored the performance of the reactive element under EMED conditions, so that it is now comparable to the performance seen under plane wave conditions. Moreover, this is seen to restore performance across the entire frequency range and no deterioration in performance is now observed for the new design. This demonstrates that it is partitioning the duct that delivers the attenuation at frequencies above the first cut-on mode in the main duct. Note, however, that this behaviour is observed for higher order modes that are cut-on in the  $y$  direction only, as this current theoretical investigation is limited to two dimensions. It is, of course, likely that in practical applications higher order modes will also cut-on in the  $z$  direction, and if this is the case then

the results obtained here indicate that this may be addressed through the use of bar silencers of the type discussed by Kirby et al. [11]. Accordingly, it is possible to use this type of hybrid reactive-dissipative approach even under more difficult acoustics conditions, such as those found in real systems that impart significant energy content into higher order modes.

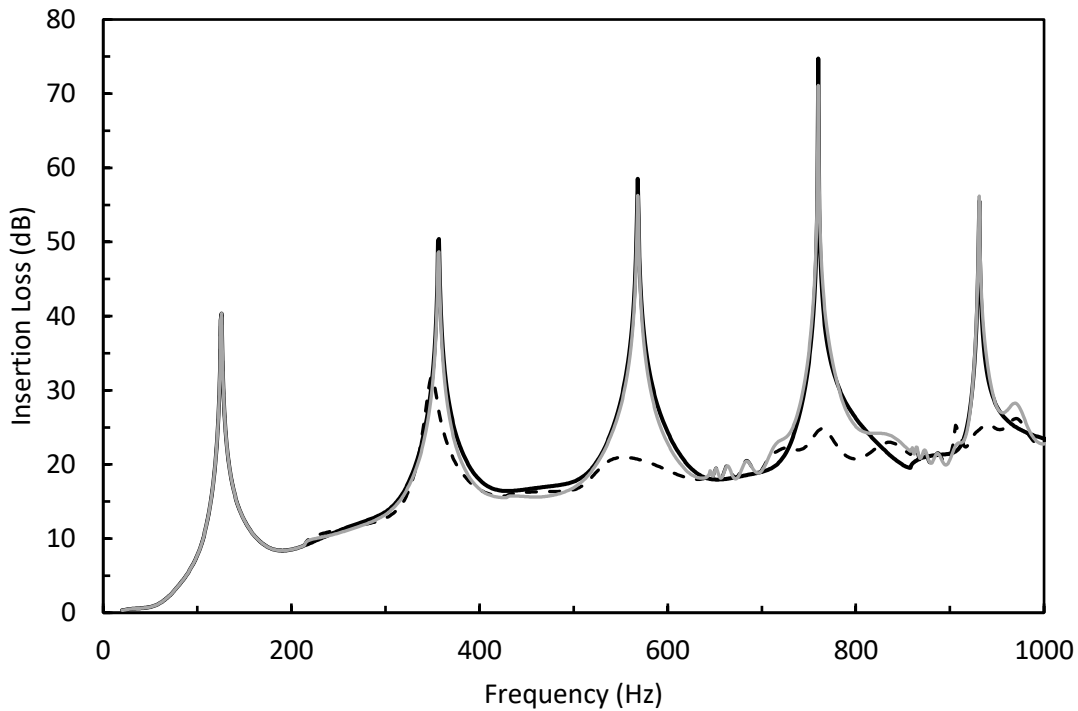


Figure 11. Comparison between predictions for a Type 1 (silencer 2) and a Type 3 (silencer 7) reactive chamber. ———, hybrid silencer 2, plane wave; - - - -, hybrid silencer 2, EMED; ———, hybrid silencer 7, EMED.

## 6. Conclusions

This article presents a new approach to delivering low to medium frequency noise control in larger ductwork that is commonly found in gas turbine systems or large HVAC applications. A new silencer design is proposed that consists of separate dissipative and reactive elements joined together to produce a new hybrid baffle design. This is intended to replace the traditional parallel dissipative splitter silencer designs that are commonly found in

larger systems, because these designs normally find it difficult to deliver the required levels of attenuation at low frequencies. Accordingly, a reactive element is used to enhance the low to medium frequency performance of the splitter silencer. However, a key requirement for the new approach to be effective is for the reactive elements to be distributed at locations across the duct, rather than placed on the duct wall. This approach is, therefore, suitable only for larger noise control applications where mean flow velocities in the main duct are relatively low.

The results presented in this article demonstrate that reactive elements are capable of delivering relatively high levels of sound attenuation over at least two low to medium frequency bands. For example, at the fundamental frequency of the reactive element, one obtains the usual resonant behaviour under plane wave conditions, and provided a sufficiently large throat area is used it is shown that acceptable levels of attenuation may be achieved over at least a  $1/3$  octave band. It is also demonstrated that the reactive elements can work at frequencies above the first and second cut-on frequencies of the duct. This is an important result, as it shows that the actions of a reactive element can be extended into the important low to medium frequency range. For instance, two different reactive chamber designs were shown to deliver increased levels of attenuation at a multiple of the chamber's fundamental frequency. Moreover, it was shown to be possible to obtain good attenuation for a reactive chamber whose fundamental frequency was above that of the first cut-on mode in the main duct. This means that it is possible to extend reactive silencer performance beyond that normally associated with designs that are placed upon the duct wall.

The reactive silencer behaviour observed here is the result of the distribution of these components across the duct so that they partition up the sound field into smaller regions. This delivers localised regions where the sound pressure field is closer to planar than in the main duct so that, even above the cut-on frequency of the first two higher order modes in the

main duct, it is possible for the reactive chambers to continue to deliver acceptable levels of sound attenuation. However, this behaviour is highly dependent on the sound pressure field inside the silencer section, and to maintain performance at higher frequencies one must ensure that a sufficient number of baffles are used to partition the duct into sufficiently small sections. Eventually the performance of the reactive elements stops in the same way as that seen when planar waves no longer propagate in traditional wall based applications.

Furthermore, the reactive chamber must also be designed to account for the properties of the incident sound field, and it is shown here that it is necessary to further partition the internal structure of a resonant chamber in order to maintain performance when the sound source contains energy propagating in higher order modes. However, provided this is accounted for, the reactive components are shown to be capable of working over an extended frequency range even when a multi-mode incident sound field is present.

A key problem with larger systems is the attenuation of low frequency noise and this has often led to the use of very large dissipative splitter silencers. This article offers an alternative approach, where the reactive element delivers low frequency attenuation rather than a dissipative element on its own, which was the case previously. The use of dissipative elements on their own has led to an over-design of splitter silencers in the medium to high frequency range, as the length was increased to deliver sufficient low frequency attenuation. The use of reactive elements now allows the dissipative elements to be optimised for the medium and high frequency range, and this allows a reduction in the length of the dissipative elements as the over-design is removed. ~~This article offers an alternative approach where the reactive element also has the potential to reduce the overall size of the dissipative element by reducing the over-design of the dissipative element.~~ Accordingly, the final size of the hybrid reactive-dissipative silencer has the potential to be significantly smaller than the equivalent dissipative silencer design. This can deliver improved noise control in restricted spaces, as



well as lower the viscous fluid losses in the duct system and so improve the efficiency of the noise source. It is also expected that the principles outlined here can be extended to other silencers designs, such as the bar silencers studied by Kirby et al. [11]. This would enable more complex tonal noise problems to be addressed by placing the reactive components at appropriate locations over the duct cross-section.

APPENDIX A

$$\begin{aligned} \mathbf{G}\mathbf{p} = & \mathbf{K}_1\mathbf{p}_1 + \mathbf{K}_2\mathbf{p}_2 + \mathbf{K}_3\mathbf{p}_3 - \mathbf{Q}_{13}\mathbf{p}_{p3} - \mathbf{Q}_{23}\mathbf{p}_{p3} - \mathbf{Q}_{31}\mathbf{p}_{p1} - \mathbf{Q}_{32}\mathbf{p}_{p2} \\ & + \mathbf{R}_{13}\mathbf{p}_{p1} + \mathbf{R}_{23}\mathbf{p}_{p2} + \mathbf{R}_{31}\mathbf{p}_{p3} + \mathbf{R}_{32}\mathbf{p}_{p3} \end{aligned} \quad (\text{A1})$$

$$\mathbf{K}_q = \int_{\Omega_q} [\nabla \mathbf{N}_q^T \nabla \mathbf{N}_q - k_q^2 \mathbf{N}_q^T \mathbf{N}_q] dx dy \quad (\text{A1})$$

$$\mathbf{Q}_{rq} = \frac{ik_0 \rho_r}{\zeta \rho_0} \int_{S_{rq}} \mathbf{N}_r^T \mathbf{N}_q dS_{rq} \quad (\text{A2})$$

$$\mathbf{R}_{rq} = \frac{ik_0 \rho_r}{\zeta \rho_0} \int_{S_{rq}} \mathbf{N}_r^T \mathbf{N}_r dS_{rq} \quad (\text{A3})$$

$$\mathbf{Q}_q = ik_0 \sum_{m=1}^{M_q} \lambda_m \int_{S_q} \phi_m \mathbf{N}_3^T dS_q \quad (\text{A4})$$

$$\mathbf{M}_q = ik_0 \sum_{m=1}^{M_q} \lambda_m \sum_{n=1}^{M_q} \int_{S_q} \phi_m \phi_n dS_q \quad (\text{A5})$$

Note that  $S_{rq}$  denotes the surface of a perforate that sits between region  $r$  and region  $q$ ; and  $\mathbf{p}_{pq}$  denotes the pressure next to the perforate in region  $\Omega_q$ . In addition,  $S_q$  denotes the vertical surface  $S_A$  or  $S_B$ , and  $\rho_q$  is the fluid density in region  $q$ , remembering that in region  $\Omega_1$  this density will be complex [14], and that  $\rho_2 = \rho_3 = \rho_0$ .

## References

1. Tyler JM, Sofrin TG. Axial flow compressor noise studies. SAE Transactions 1962; 70: 309-332.
2. Morfey, CL. Rotating blades and aerodynamic sound. Journal of Sound and Vibration 1973; 28: 587-617.
3. Seo SH, Kim YH. Silencer design by using array resonators for low-frequency band noise reduction. Journal of the Acoustical Society of America 2005; 118(4): 2332–2338.
4. Cai C, Mak CM. Noise control zone for a periodic ducted Helmholtz resonator system. Journal of the Acoustical Society of America 2016; 140: EL471-EL477.
5. Glav R, Regaud P-L, Åbom M. Study of folded resonator including the effects of higher order modes. Journal of Sound and Vibration 2004; 273: 777-792.
6. Tang SK. Narrow sidebranch arrays for low frequency duct noise control. Journal of the Acoustical Society of America 2012; 132(4): 3086–3097.
7. Kirby R. The influence of baffle fairings on the acoustic performance of rectangular splitter silencers. Journal of the Acoustical Society of America 2005; 118: 2302-2312.
8. Kirby R, Lawrie JB. A point collocation approach to modelling large dissipative silencers. Journal of Sound and Vibration 2005; 286: 313-339.
9. Zhou Z, Wu TW, Ruan K, Herrin DW. A reciprocal identity method for large silencer analysis. Journal of Sound and Vibration 2016; 364: 165-176.
10. Wang P, Wu TW. Impedance-to-scattering matrix method for large silencer analysis using direct collocation. Engineering Analysis with Boundary Elements 2016; 73: 191-199.

11. Kirby R, Williams PT, Hill J. A three dimensional investigation into the acoustic performance of dissipative splitter silencers. *Journal of the Acoustical Society of America* 2014; 135: 2727-2737.
12. Yang L, Wang P, Wu TW. Boundary element analysis of bar silencers using the scattering matrix with two dimensional finite element modes. *Engineering Analysis with Boundary Elements* 2017; 74: 100-106.
13. Selamet A, Lee, IJ, Huff NT. Acoustic attenuation of hybrid silencers. *Journal of Sound and Vibration* 2003; 262: 509-527.
14. Denia FD, Selamet A, Fuenmayor FJ, Kirby R. Acoustic attenuation performance of perforated dissipative mufflers with empty inlet/outlet extensions. *Journal of Sound and Vibration* 2007; 302: 1000-1017.
15. Lee IJ, Selamet A, Huff NT, Hrdlicka M. Design of a hybrid exhaust silencing system for a production engine. *SAE Noise and Vibration Conference and Exhibition* 2005; May 16-19, Paper 85953.
16. Papini GS, Pinto RLUF, Medeiros EB, Coelho FBG. Hybrid approach to noise control of industrial exhaust systems. *Applied Acoustics* 2017; 125: 102-212.
17. Kirby R, Amott K, Williams PT, Duan W. On the acoustic performance of rectangular splitters in the presence of mean flow. *Journal of Sound and Vibration* 2014; 333: 6295-6311.
18. Kirby R. A comparison between analytic and numerical methods for modelling automotive dissipative silencers with mean flow. *Journal of Sound and Vibration* 2009; 325: 565-582.
19. Mechel FP. Theory of baffle-type silencers. *Acustica* 1990; 70: 93-111.

20. European Standard EN ISO 29053: Materials for acoustical applications: determination of airflow resistance. 1993.
21. Kirby R. On the modification of Delany and Bazley formulae. *Applied Acoustics* 2014; 86: 47-49.
22. Kirby R, Cummings A. The impedance of perforated plates subjected to grazing mean flow and backed by porous media. *Journal of Sound and Vibration* 1998; 217: 619-636.